BMJ open

Cross-sectional study: Does combining optical coherence tomography measurements using the 'Random Forest' decision tree classifier improve the prediction of the presence of perimetric deterioration in glaucoma suspects?

Koichiro Sugimoto,[1] Hiroshi Murata,[1] Hiroyo Hirasawa,[1] Makoto Aihara,[1,2] Chihiro Mayama,[1] Ryo Asaoka[1]

To cite: Sugimoto K, Murata H, Hirasawa H, *et al*. Cross-sectional study: Does combining optical coherence tomography measurements using the 'Random Forest' decision tree classifier improve the prediction of the presence of perimetric deterioration in glaucoma suspects?. *BMJ Open* 2013;**3**: e003114. doi:10.1136/bmjopen-2013-003114

▸ Prepublication history and additional material for this paper is available online. To view these files please visit the journal online (http://dx.doi.org/10.1136/bmjopen-2013-003114).

Received 24 April 2013
Revised 20 June 2013
Accepted 12 August 2013

[1]Department of Ophthalmology, Graduate School of Medicine, The University of Tokyo, Tokyo, Japan
[2]Shirato Eye Clinic, Tokyo, Japan

Correspondence to
Dr Ryo Asaoka;
rasaoka-tky@umin.ac.jp

ABSTRACT

Objectives: To develop a classifier to predict the presence of visual field (VF) deterioration in glaucoma suspects based on optical coherence tomography (OCT) measurements using the machine learning method known as the 'Random Forest' algorithm.

Design: Case–control study.

Participants: 293 eyes of 179 participants with open angle glaucoma (OAG) or suspected OAG.

Interventions: Spectral domain OCT (Topcon 3D OCT-2000) and perimetry (Humphrey Field Analyser, 24-2 or 30-2 SITA standard) measurements were conducted in all of the participants. VF damage (Ocular Hypertension Treatment Study criteria (2002)) was used as a 'gold-standard' to classify glaucomatous eyes. The 'Random Forest' method was then used to analyse the relationship between the presence/absence of glaucomatous VF damage and the following variables: age, gender, right or left eye, axial length plus 237 different OCT measurements.

Main outcome measures: The area under the receiver operating characteristic curve (AROC) was then derived using the probability of glaucoma as suggested by the proportion of votes in the Random Forest classifier. For comparison, five AROCs were derived based on: (1) macular retinal nerve fibre layer (m-RNFL) alone; (2) circumpapillary (cp-RNFL) alone; (3) ganglion cell layer and inner plexiform layer (GCL +IPL) alone; (4) rim area alone and (5) a decision tree method using the same variables as the Random Forest algorithm.

Results: The AROC from the combined Random Forest classifier (0.90) was significantly larger than the AROCs based on individual measurements of m-RNFL (0.86), cp-RNFL (0.77), GCL+IPL (0.80), rim area (0.78) and the decision tree method (0.75; $p<0.05$).

Conclusions: Evaluating OCT measurements using the Random Forest method provides an accurate prediction of the presence of perimetric deterioration in glaucoma suspects.

SUMMARY

Strengths and limitations of this study

- Combining optical coherence tomography measurements.
- Accurate prediction of the presence of perimetric deterioration in glaucoma suspects.
- Lack of a normative population to act as a reference.

INTRODUCTION

Glaucoma is the second most common cause of blindness. As glaucomatous visual field (VF) damage is irreversible, the early diagnosis of glaucoma is essential. Structural changes at the optic nerve head[1] and retinal nerve fibre layer (RNFL) around the optic disc[2] can also indicate glaucomatous damage and may precede measurable VF loss.

Optical coherence tomography (OCT) is an imaging technology widely used in the diagnosis of glaucoma, enabling high-resolution measurements of the retina.[3] The recent advancement of OCT from the time domain to the spectral domain OCT (SD-OCT) has greatly improved the imaging speed and resolution of the device,[4] and has enabled imaging scans of the macular RNFL (m-RNFL) and the macular ganglion cell layer and inner plexiform layer (GCL+IPL). It has been reported that these retinal layers are damaged early in the glaucoma disease process[5 6] and many studies have investigated the diagnostic performance of thickness measurements of these structures to discriminate between healthy and glaucomatous eyes.[7–14] However, in these previous studies, the different measurements were interpreted independently, yet damage to

these structures does not necessarily occur in parallel[15 16] and thus there is no consensus on which structure is optimum for diagnosing glaucoma. Indeed, specific structures may be preferentially damaged in any given patient. For example, Cordeiro *et al*[17] reported that the diagnostic performance of circumpapillary RNFL (cp-RNFL) thickness measurements tended to be better in patients with a small optic disc, and an inverse effect was observed using the macular ganglion cell complex (GCC) measurement. Conversely, GCC may be preferential to detect glaucomatous change in patients with high myopia.[18] Thus, it appears that no single structural measurement is best for diagnosing glaucoma.

The 'Random Forest' method is a decision support tool which consists of many decision trees. Decision trees have previously been used to diagnose glaucoma[19]; however, decision trees suffer from the problem of 'overfitting', which influences the diagnostic accuracy.[20] On the contrary, the Random Forest classifier overcomes this problem by summarising the results of many decision trees. Another noteworthy advantage of the Random Forest algorithm over traditional methods, such as logistic regression, is that any interaction or correlation between variables does not adversely affect the classification since it is capable of representing high-order interactions.[21] Furthermore, predictors that might otherwise be masked by their correlation with other variables, using other classification methods, can contribute to the Random Forest classifier.

Glaucomatous structural change is often apparent in patients with glaucoma without VF defects (preperimetric glaucoma).[22 23] Therefore, it may be possible to predict the presence of the VF deterioration from structural measurements, as it has been reported that there is a significant difference in structural measurements between patients with perimetric and preperimetric glaucoma.[22] Predicting the presence of VF damage from structural measurements is clinically very important, especially in patients who cannot reliably perform VF test, for example, due to inability to concentrate, mental disorders, locomotor disabilities, etc. The purpose of this study was to improve the prediction of the presence of VF damage in glaucoma suspects by analysing multiple OCT measurements concurrently using the Random Forest algorithm.

MATERIALS AND METHODS

Written consent was given by the patients for their information to be stored in the hospital database and used for research. This study was performed according to the tenets of the Declaration of Helsinki.

This retrospective study comprised 293 eyes of 179 consecutive patients referred to the University of Tokyo Hospital for glaucoma or suspected glaucoma between August 2010 and July 2012. Patients were referred based on optic disc damage: focal or diffuse neuroretinal rim thinning, localised notching or nerve fibre layer defects. The patients underwent complete ophthalmic examinations, including slit lamp biomicroscopy, gonioscopy, intraocular pressure measurement and funduscopy. If glaucomatous structural changes were confirmed from these tests, axial length (AL; IOL Master, Carl Zeiss Meditec, Dublin, California, USA), imaging with SD-OCT and VF testing were performed. The criteria for inclusion were visual acuity better than 6/12; no previous ocular surgery, except cataract extraction and intraocular lens implantation; open anterior chamber angle (patients with angle closure glaucoma and secondary open angle glaucoma were excluded); no other anterior and posterior segment eye disease. AL was not used for the inclusion/exclusion criteria.

VF testing was performed using the Humphrey Field Analyzer (HFA, Carl Zeiss Meditec), 24-2 or 30-2 test pattern and the Swedish interactive threshold algorithm (SITA) Standard strategy, with the Goldmann size III target. Near refractive correction was used as necessary, calculated according to the patient's age by the HFA software. Unreliable VFs were excluded according to the HFA criteria (fixation losses greater than 25%, or false-positive responses greater than 15%). A false negative rate was not used as an indicator of test reliability following a previous report.[24] A glaucomatous VF was defined as a pattern SD value beyond the normal limit ($p<0.05$), or a Glaucoma Hemifield Test result outside normal limits following the criteria in.[25] All patients with glaucoma had previous experience in visual field testing.

SD-OCT (3D OCT-2000; Topcon Corp, Tokyo, Japan) was used to obtain tomographic images of the parapapillary fundus with the three-dimensional (3D) disc scan and 3D Macula scan (128 horizontal scan lines comprised of 512 A scans for an image area of 6×6 mm). SD-OCT uses a superluminescent diode laser with a centre wavelength of 840 nm and a bandwidth of 50 nm as the light source. The transverse and axial resolutions are less than 20 and 5 µm, respectively. The acquisition speed is 50 000 A scans/s. In the selected eye, the macula was imaged by six radial lines centred at the fovea spaced 30° apart. All of the measurements were performed after pupil dilation with 1% Tropicamide and all of the images had signal strength of at least 60, as recommended by the manufacturer.

The 'Random Forest' algorithm is an ensemble machine learning classifier proposed by Breiman in 2001.[26 27] The Random Forest consists of many decision trees and outputs the class that is the mode of the classes output by individual trees. Thus, the Random Forest is an ensemble classifier, which has been reported to improve the prediction accuracy of decision tree.[28] Indeed there are many reports that suggest that the Random Forest gives the best prediction accuracy among various machine learning methods and it has been used in many research fields, including gene selection and cancer classification.[29–32] In the Random Forest method, when classifying a new object from an input vector, the input vector is classified by each of the trees in the

forest and the tree 'votes' for that class. The forest then chooses the classification having the most votes over all the trees in the forest. Each tree is constructed using a different bootstrap sample from the original data. Thus, cross-validation is performed internally and there is no need for a separate cross-validation data set to obtain an unbiased estimate of the test set error. For classification, node impurity was measured using the Gini index.[33]

The Random Forest method was used to classify the presence or absence of glaucomatous VF damage using: OCT measurements (237 different measurements in total were analysed), age, gender, AL and right/left eye (see table 1). In this procedure, 10 000 trees were grown and 5 among the 241 parameters were used at each node. The area under the receiver operating characteristic curve (AROC) was derived from the probability of glaucoma (the proportion of votes) as suggested by the method; for each individual, only the data from all other participants (n=178) was used (leave-one-out cross validation) so that right and left eyes of a participant were not used for training and testing simultaneously. For comparison, the AROCs were also derived using only individual raw thickness measurements of: m-RNFL, or cp-RNFL, or GCL+IPL, or rim area and the prediction with the decision tree method. The diagnostic sensitivity and specificity was also calculated for the age-matched normative limits of the different measurements ($p \leq 5\%$ or $p \leq 1\%$): m-RNFL and GCL+IPL, as shown on the instrument's print out.

Table 1 The variables used in the analysis, including 237 optical coherence tomography parameters

Measurement	
cp-RNFL	Total, 4 sectors (superior, temporal, nasal, inferior), 12 sectors
m-RNFL	Total, 2 sectors (superior, inferior), 100 sectors
GCL+IPL	Total, 2 sectors (superior, inferior), 100 sectors
Optic disc	Disc area, cup area, rim area, cup volume, rim volume, C/D area ratio, linear C/D ratio, vertical C/D ratio, disc diameter (vertical), disc diameter (horizontal)
m-RNFL	Significant according to normative database (p value <5%)
m-RNFL	Significant according to normative database (p value <1%)
GCL+IPL	Significant according to normative database (p<5%)
GCL+IPL	Significant according to normative database (p value <1%)
Age	
Gender	
AL	
Eye (right/left)	

AL, axial length; cp-RNFL, circumpapillary retinal nerve fibre layer; GCL+IPL, ganglion cell layer and inner plexiform layer; m-RNFL, macular RNFL.

Finally, variable importance was calculated by randomly permuting a variable at each decision tree and observing whether the number of correct decisions decreased.[27]

All statistical analyses were carried out using the statistical programming language R (V.2.14.2, The R Foundation for Statistical Computing, Vienna, Austria) and Medcalc V.11.4.2.0; MedCalc statistical software, Mariakerke, Belgium). The R package 'randomForest' and 'rpart' was used to carry out the analysis of the Random Forest method and decision tree method, respectively.

RESULTS

Participant's characteristics are given in table 2. VFs of 224 eyes in 150 patients were diagnosed as glaucomatous while the remaining 69 eyes of 57 patients were judged as normal. The average total m-RNFL thickness, cp-RNFL thickness, GCL+IPL thickness and rim area were significantly smaller in the glaucomatous group compared with the normal group ($p<0.05$, non-paired t test).

As shown in the figure 1, the AROC of the Random Forest method utilising all measurements (0.90) was significantly larger than that with m-RNFL alone (0.86), cp-RNFL alone (0.77), GCL-IPL (0.80) and rim area alone (0.78; $p<0.05$). Furthermore, the diagnostic performance (sensitivity and specificity) of the age-matched normative database (as shown on the OCT printout) were also plotted in figure 1. The sensitivity and specificity for thickness values outside normal limits were: m-RNFL ($p<5\%$): 0.74 and 0.93; m-RNFL ($p<1\%$): 0.61 and 0.96; GCL+IPL ($p<5\%$): 0.48 and 0.88; GCL+IPL ($p<1\%$): 0.42 and 0.90 (sensitivity and specificity, respectively).

Figure 2 illustrates the OCT measurements analysed. Among 237 measurements, 76 had a significant variable importance measure including: total and inferior m-RNFL thickness, total and inferior GCL+IPL thickness, an m-RNFL thickness value outside normal limits ($p<5\%$), various sectorial m-RNFL thickness values (figure 2A), various GCL+IPL thickness values (figure 2B) and two cp-RNFL thickness values (figure 2A). Age, AL, gender and right or left eye were not significant.

DISCUSSION

In the current study, the 'Random Forest' decision tree classifier was used to predict the presence of VF damage in glaucoma suspects. As a result, it was shown that the AROC given by the Random Forest method was significantly larger than those derived from any single OCT parameter and the simple decision tree method.

Previous attempts have been made to interpret multiple structural parameters in order to aid the diagnosis of glaucoma. Chen *et al* used a logistical diagnostic model to diagnose glaucoma; the model analysed a patient's optic cup:optic disc vertical ratio, cp-RNFL thickness and rim area simultaneously, but the authors

Table 2 Characteristics of the study participants

	'Glaucomatous' VF group			'Normal' VF group			
	Mean	SD	Range	Mean	SD	Range	p Value
Age (years)	53.6	13.2	17–85	48.5	12.7	17–48	<0.01
MD (dB)	−6.2	5.2	−28.2–1.8	−0.5	1.2	−3.6–1.3	<0.01
AL (mm)	25.1	1.7	22.2–29.3	26.0	1.0	22.8–29.5	0.11
m-RNFL (μm)	25.5	7.9	1.0–46.6	35.6	5.4	27.5–63.1	<0.01
cp-RNFL (μm)	88.3	15.1	49.0–123.4	104.0	15.0	66.9–150.9	<0.01
GCL+IPL (μm)	68.8	15.3	43.7–106.5	89.3	19.7	55.7–127.3	<0.01
Rim area (mm^2)	1.1	0.5	0.3–3.8	1.6	0.6	0.6–3.7	<0.01
Eye (right/left)	116/108			35/34			
Gender (male/female)	108/116			38/31			

AL, axial length; cp-RNFL, circumpapillary retinal nerve fibre layer; GCL+IPL, ganglion cell layer and inner plexiform layer; MD, mean deviation; m-RNFL, macular; VF, visual field.

found that diagnostic performance was not significantly improved compared with using individual measurements.[34] On the other hand, Burgansky-Eliash *et al*[35] used a support vector machine classifier of multiple Stratus OCT parameters to diagnose glaucoma and showed that the AROC was significantly larger. Other studies also support combining multiple structural measurements to diagnose glaucoma.[36 37] In addition, a recent study suggested the decision tree method is useful to discriminate between patients with glaucoma and normal participants.[19] However, in the current study, the decision tree method, which often suffers from the problem of over-fitting,[38] failed to show benefit in discriminating glaucoma. On the other hand, it was beneficial to use the Random Forest method, which is an ensemble classifier of decision trees. Recent reports have revealed that distinguishing between perimetric glaucoma and preperimetric glaucoma is more difficult than differentiating normal participants from patients with glaucoma[39] with early VF damage.[22] A noteworthy advantage of the current study is that it is the first of its kind to analyse m-RNFL and GCL+IPL layers simultaneously with cp-RNFL, optic disc shape parameters as well age and AL.

It must be noted that a clear caveat of the current study is the lack of a normative population to act as a reference. Therefore, AROCs derived in the current study are not directly relevant to distinguishing between healthy participants and patients with glaucoma. A further study should be carried out with normative and glaucomatous populations (particularly patients with early stage glaucoma) in order to further investigate the merits of the Random Forest classifier. Nonetheless, the method's ability to accurately differentiate glaucoma

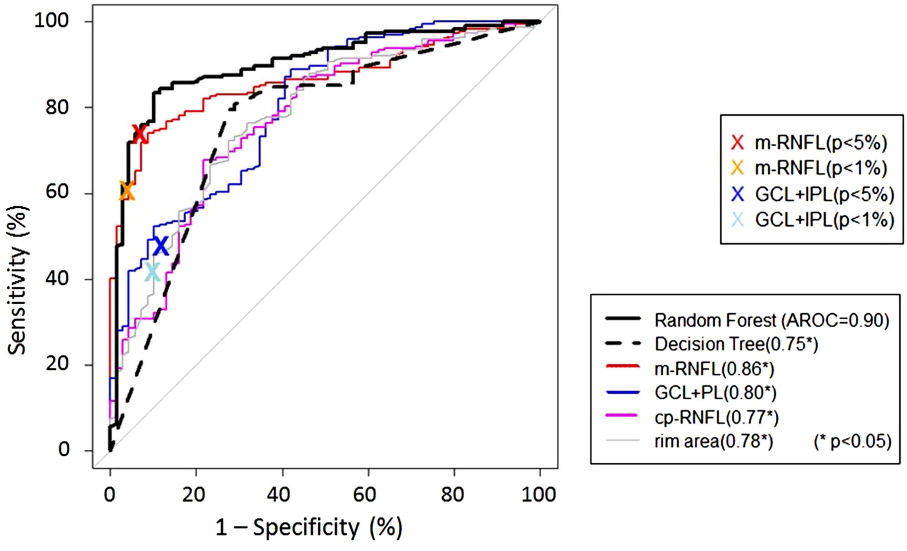

Figure 1 ROC curves with the probability of glaucoma suggested by the Random Forest classifier and raw thickness measurements of: m-RNFL alone, cp-RNFL alone, and GCL+IPL alone, and decision tree method. The area under the ROC with the Random Forest method was significantly larger than those of individual measurements and decision tree method (p<0.05). The coloured 'X' represent the sensitivity and specificity of the SD-OCT normative database (red: m-RNFL (p<5%), orange: m-RNFL (p<1%), green: GCL+IPL (p<5%), blue: GCL+IPL (p<1%)). AL, axial length; cp-RNFL, circumpapillary retinal nerve fibre layer; GCL+IPL, ganglion cell layer and inner plexiform layer; m-RNFL, macular RNFL; ROC, receiver operating characteristic.

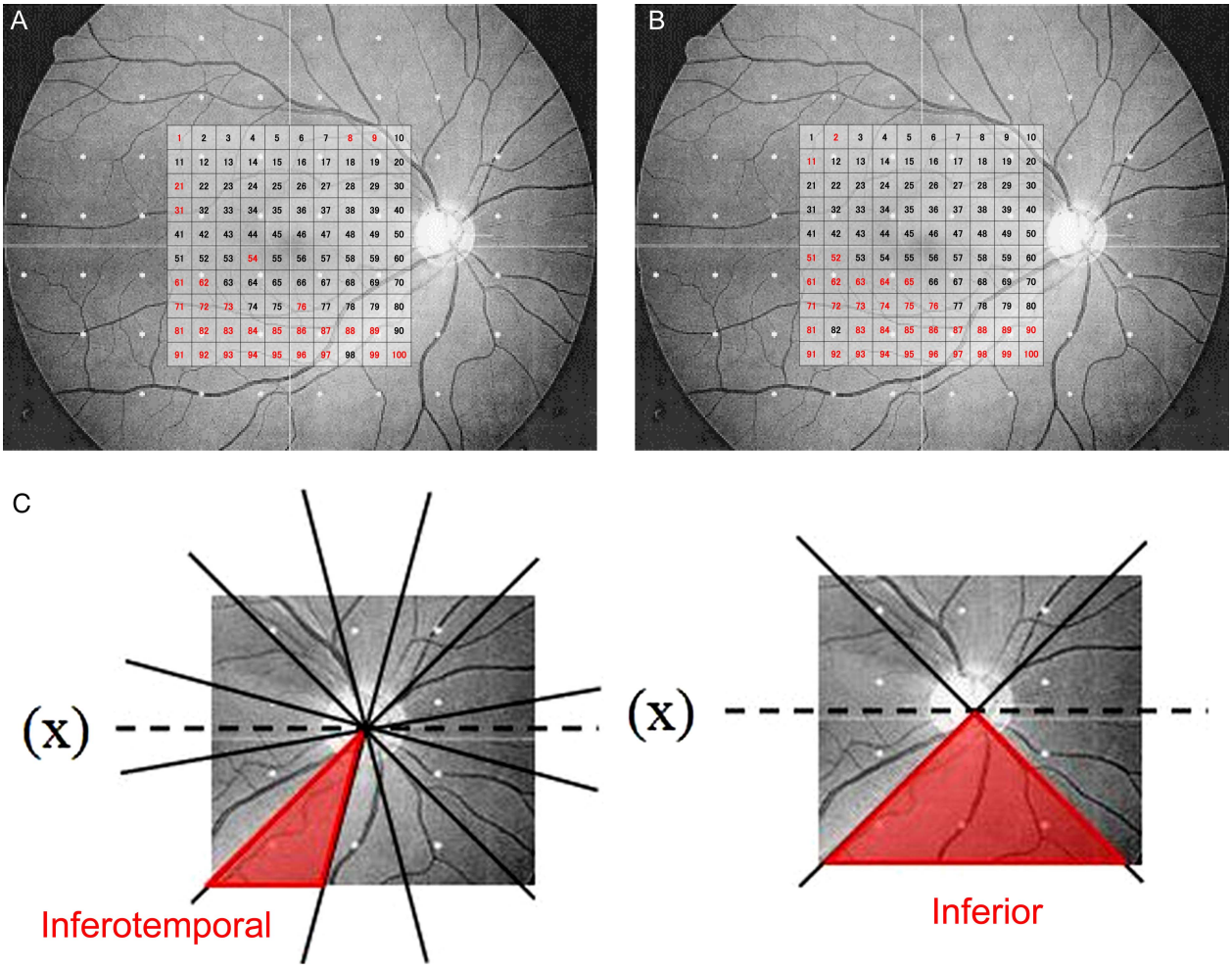

Figure 2 Variables in the Random Forest classifier having a significant effect on the presence of glaucomatous visual field damage. Sectors of the cp-RNFL, m-RNFL and GCL+IPL were superimposed onto a fundus photograph[44]; significant sectors are highlighted in red. If a participant's left eye was tested, the recorded data were mapped to a right eye format for analysis. (A) cp-RNFL, (B): m-RNFL, (C): GCL+IPL. AL, axial length; cp-RNFL, circumpapillary retinal nerve fibre layer; GCL+IPL, ganglion cell layer and inner plexiform layer; m-RNFL, macular RNFL.

suspects from patients with glaucoma suggests that the classifier may be even more useful in this context.

The variable importance measure from the Random Forest method suggested that total m-RNFL thickness, total GCL+IPL thickness and m-RNFL thickness outside normal limits (p<5%) significantly contributed to the diagnosis of glaucoma. In contrast, age, AL, gender, eye (right/left) and optic disc measurements such as rim area, were not significant. Reports have suggested that optic disc shape parameters are useful for classifying glaucomatous eyes, but are less useful compared to RNFL parameters.[16 40] However, previous results have been based on Heidelberg retina tomography (HRT) measurements of the optic disc and there are notable differences between the corresponding measurements in SD-OCT. For instance, the margin of the optic disc and cup is automatically identified in SD-OCT, whereas it is manually drawn by the examiner in HRT. Furthermore, it has been reported that HRT measurements of optic disc shape detect a different population of patients with glaucoma to OCT measurements of the RNFL.[16] Accordingly, the diagnostic performance of the Random Forest classifier may be further improved by also including various optic disc-shape parameters derived from HRT. We intend to investigate this hypothesis in a future study.

Interestingly, our results question the validity of SD-OCT's normal limits to discriminate glaucoma. For example, the blue cross in figure 1 indicates that GCL +IPL measurements outside normal limits at the p<1% level have a specificity of 90%. The normal limits of the SD-OCT are derived by testing 'normal' participants without ocular disease; Rao *et al*[41] have reported that cp-RNFL thickness measurements from normal participants and patients with glaucoma overlap considerably. A significant advantage of the Random Forest classifier is that normal limits could be established based on results from normal participants and patients with glaucoma; these would be expected to better reflect the 'true' specificity of the test result. Another merit of the Random Forest method, in comparison to the current

standard, is that the method gives an exact probability of glaucoma, rather than a binary classification (glaucoma or not at p<1%, or p<5%); such a value could be interpreted in a manner similar to that of the 'Nerve Fiber Index' score in the nerve fibre analyser imaging instrument (GDx, Carl Zeiss Meditec), which is a continuous numeric score from 0 to 99.

In our Random Forest classifier, many sectorial thickness measurements of the m-RNFL, GCL+IPL and cp-RNFL layers were deemed significant for the prediction of glaucomatous VF damage. Significant sectors were generally located in the inferior hemiretina, although a few sectors were also situated in the superior hemiretina (see figure 2). Previous studies have suggested that glaucomatous VF damage preferably affects the superior hemifield.[42 43] Interestingly, the significant m-RNFL, GCL+IPL and cp-RNFL sectors in our classifier were principally distributed along the inferotemporal RNFL bundle, which likely corresponds to an arcuate defect in the superior VF.[44] Thus, these results also suggest that glaucomatous RNFL/GCL+IPL damage tends to occur in the inferior hemiretina.

OCT structural measurements are influenced by ageing; cp-RNFL,[45–47] rim area,[48] m-RNFL and GCL+IPL all become thinner with age.[49] In addition, studies suggest that AL may have an effect on measurements of the cp-RNFL,[48 50] rim area,[48 50] m-RNFL[49] and GCL+IPL[49]; however any such effects remain contentious.[51–53] In our study, removing age and AL factors did not affect the AROC of the Random Forest classifier.

Other machine learning methods, such as support vector machines, boosting and bagging classifiers could also be used to diagnose glaucoma. Previous reports suggest that the Random Forest method outperforms most other methods[31 54 55]; hence the Random Forest algorithm was used in the current study. Nevertheless, in a future study, we intend to investigate the performance of machine learning methods for discriminating perimetric and preperimetric glaucoma.

In conclusion, we have shown that combining SD-OCT measurements of the m-RNFL, cp-RNFL, GCL+IPL layers, using the Random Forest method, is beneficial for predicting the presence of glaucomatous VF damage in glaucoma suspects, especially when compared with the current OCT reference-standard of comparing these measurements to an age-matched normative database.

Acknowledgements The authors express huge thanks to Hiroyo Hirasawa for her invaluable help with manuscript preparation and publication.

Contributors MA and CM gave advice from the viewpoint of a glaucoma specialist. KS, HM and RA conceived and designed the experiments, performed the experiments, analysed the data, contributed in arranging reagents/materials/analysis tools and wrote the manuscript.

Funding This research was supported in part by grants 25861618 (HM), 60645000 (HH), and 50570701 (CM) from the Ministry of Education, Culture, Sports, Science and Technology of Japan.

Competing interests None.

Ethics approval The study was approved by the Research Ethics Committee of the Graduate School of Medicine and Faculty of Medicine at the University of Tokyo.

Provenance and peer review Not commissioned; externally peer reviewed.

Data sharing statement No additional data are available.

REFERENCES

1. Quigley HA, Katz J, Derick RJ, *et al*. An evaluation of optic disc and nerve fiber layer examinations in monitoring progression of early glaucoma damage. *Ophthalmology* 1992;99:19–28.
2. Sommer A, Katz J, Quigley HA, *et al*. Clinically detectable nerve fiber atrophy precedes the onset of glaucomatous field loss. *Arch Ophthalmol* 1991;109:77–83.
3. Chang R, Budenz DL. New developments in optical coherence tomography for glaucoma. *Curr Opin Ophthalmol* 2008;19:127–35.
4. Huang D, Swanson EA, Lin CP, *et al*. Optical coherence tomography. *Science* 1991;254:1178–81.
5. Quigley HA, Dunkelberger GR, Green WR. Retinal ganglion cell atrophy correlated with automated perimetry in human eyes with glaucoma. *Am J Ophthalmol* 1989;107:453–64.
6. Nakano N, Ikeda HO, Hangai M, *et al*. Longitudinal and simultaneous imaging of retinal ganglion cells and inner retinal layers in a mouse model of glaucoma induced by N-methyl-D-aspartate. *Invest Ophthalmol Vis Sci* 2011;52:8754–62.
7. Cho JW, Sung KR, Lee S, *et al*. Relationship between visual field sensitivity and macular ganglion cell complex thickness as measured by spectral-domain optical coherence tomography. *Invest Ophthalmol Vis Sci* 2010;51:6401–7.
8. Garas A, Vargha P, Hollo G. Diagnostic accuracy of nerve fibre layer, macular thickness and optic disc measurements made with the RTVue-100 optical coherence tomograph to detect glaucoma. *Eye* 2011;25:57–65.
9. Kim NR, Lee ES, Seong GJ, *et al*. Structure-function relationship and diagnostic value of macular ganglion cell complex measurement using Fourier-domain OCT in glaucoma. *Invest Ophthalmol Vis Sci* 2010;51:4646–51.
10. Moreno PA, Konno B, Lima VC, *et al*. Spectral-domain optical coherence tomography for early glaucoma assessment: analysis of macular ganglion cell complex versus peripapillary retinal nerve fiber layer. *Can J Ophthalmol* 2011;46:543–7.
11. Rao HL, Babu JG, Addepalli UK, *et al*. Retinal nerve fiber layer and macular inner retina measurements by spectral domain optical coherence tomograph in Indian eyes with early glaucoma. *Eye* 2012;26:133–9.
12. Rao HL, Kumbar T, Addepalli UK, *et al*. Effect of spectrum bias on the diagnostic accuracy of spectral-domain optical coherence tomography in glaucoma. *Invest Ophthalmol Vis Sci* 2012;53:1058–65.
13. Schulze A, Lamparter J, Pfeiffer N, *et al*. Diagnostic ability of retinal ganglion cell complex, retinal nerve fiber layer, and optic nerve head measurements by Fourier-domain optical coherence tomography. *Graefes Arch Clin Exp Ophthalmol* 2011;249:1039–45.
14. Tan O, Chopra V, Lu AT, *et al*. Detection of macular ganglion cell loss in glaucoma by Fourier-domain optical coherence tomography. *Ophthalmology* 2009;116:2305–14. e1–2.
15. Tuulonen A, Lehtola J, Airaksinen PJ. Nerve fiber layer defects with normal visual fields. Do normal optic disc and normal visual field indicate absence of glaucomatous abnormality? *Ophthalmology* 1993;100:587–97; discussion 97–8.
16. Leung CK, Choi N, Weinreb RN, *et al*. Retinal nerve fiber layer imaging with spectral-domain optical coherence tomography: pattern of RNFL defects in glaucoma. *Ophthalmology* 2010;117:2337–44.
17. Cordeiro DV, Lima VC, Castro DP, *et al*. Influence of optic disc size on the diagnostic performance of macular ganglion cell complex and peripapillary retinal nerve fiber layer analyses in glaucoma. *Clini Ophthalmol* 2011;5:1333–7.
18. Shoji T, Nagaoka Y, Sato H, *et al*. Impact of high myopia on the performance of SD-OCT parameters to detect glaucoma. *Graefes Arch Clin Exp Ophthalmol* 2012;250:1843–9.
19. Baskaran M, Ong EL, Li JL, *et al*. Classification algorithms enhance the discrimination of glaucoma from normal eyes using

high-definition optical coherence tomography. *Invest Ophthalmol Vis Sci* 2012;53:2314–20.
20. Mitchell T. *Machine learning*. McGraw-Hill Higher Education, 1997.
21. Strobl C, Boulesteix AL, Kneib T, *et al*. Conditional variable importance for random forests. *BMC Bioinformatics* 2008;9:307.
22. Cvenkel B, Kontestabile AS. Correlation between nerve fibre layer thickness measured with spectral domain OCT and visual field in patients with different stages of glaucoma. *Graefes Arch Clin Exp Ophthalmol* 2011;249:575–84.
23. Jeoung JW, Park KH. Comparison of Cirrus OCT and Stratus OCT on the ability to detect localized retinal nerve fiber layer defects in preperimetric glaucoma. *Invest Ophthalmol Vis Sci* 2010;51:938–45.
24. Bengtsson B, Heijl A. False-negative responses in glaucoma perimetry: indicators of patient performance or test reliability? *Invest Ophthalmol Vis Sci* 2000;41:2201–4.
25. Gordon MO, Beiser JA, Brandt JD, *et al*. The Ocular Hypertension Treatment Study: baseline factors that predict the onset of primary open-angle glaucoma. *Arch Ophthalmol* 2002;120:714–20. discussion 829–30.
26. Breiman L. Random Forests. *Mach Learn* 2001;45:5–32.
27. Breiman L, Cutler A. Random Forests. 2004. http://www.stat.berkeley.edu/~breiman/RandomForests/cc_home.htm
28. Dietterich TG. Ensemble learning. In: *The handbook of brain theory and neural networks*. 2nd edn. Cambridge: The MIT Press, 2002.
29. Palmer DS, O'Boyle NM, Glen RC, *et al*. Random forest models to predict aqueous solubility. *J Chem Inf Model* 2007;47:150–8.
30. Wu B, Abbott T, Fishman D, *et al*. Comparison of statistical methods for classification of ovarian cancer using mass spectrometry data. *Bioinformatics* 2003;19:1636–43.
31. Diaz-Uriarte R, Alvarez de Andres S. Gene selection and classification of microarray data using random forest. *BMC Bioinformatics* 2006;7:3.
32. Svetnik V, Liaw A, Tong C, *et al*. Random forest: a classification and regression tool for compound classification and QSAR modeling. *J Chem Inf Comput Sci* 2003;43:1947–58.
33. Gini C. 1909 Concentration and dependency ratios (in Italian). *Riv Pol Econ* 1997;87:769–89.
34. Fang Y, Pan YZ, Li M, *et al*. Diagnostic capability of Fourier-Domain optical coherence tomography in early primary open angle glaucoma. *Chin Med J* 2010;123:2045–50.
35. Burgansky-Eliash Z, Wollstein G, Chu T, *et al*. Optical coherence tomography machine learning classifiers for glaucoma detection: a preliminary study. *Invest Ophthalmol Vis Sci* 2005;46:4147–52.
36. Lu AT, Wang M, Varma R, *et al*. Combining nerve fiber layer parameters to optimize glaucoma diagnosis with optical coherence tomography. *Ophthalmology* 2008;115:1352–7, 57e1–2.
37. Chen HY, Huang ML, Hung PT. Logistic regression analysis for glaucoma diagnosis using Stratus Optical Coherence Tomography. *Optom Vis Sci* 2006;83:527–34.
38. Hastie T, Tibshirani R, Friedman J. *The elements of statistical learning*. New York: Springer, 2001.
39. Morooka S, Hangai M, Nukada M, *et al*. Wide 3-dimensional macular ganglion cell complex imaging with spectral-domain optical coherence tomography in glaucoma. *Invest Ophthalmol Vis Sci* 2012;53:4805–12.
40. Lisboa R, Leite MT, Zangwill LM, *et al*. Diagnosing preperimetric glaucoma with spectral domain optical coherence tomography. *Ophthalmology* 2012.
41. Rao HL, Zangwill LM, Weinreb RN, *et al*. Comparison of different spectral domain optical coherence tomography scanning areas for glaucoma diagnosis. *Ophthalmology* 2010;117:1692–9, 99e1.
42. Hart WM Jr, Becker B. The onset and evolution of glaucomatous visual field defects. *Ophthalmology* 1982;89:268–79.
43. Heijl A, Lundqvist L. The frequency distribution of earliest glaucomatous visual field defects documented by automatic perimetry. *Acta Ophthalmol* 1984;62:658–64.
44. Garway-Heath DF, Poinoosawmy D, Fitzke FW, *et al*. Mapping the visual field to the optic disc in normal tension glaucoma eyes. *Ophthalmology* 2000;107:1809–15.
45. Lee JY, Hwang YH, Lee SM, *et al*. Age and retinal nerve fiber layer thickness measured by spectral domain optical coherence tomography. *Korean J Ophthalmol* 2012;26:163–8.
46. Parikh RS, Parikh SR, Sekhar GC, *et al*. Normal age-related decay of retinal nerve fiber layer thickness. *Ophthalmology* 2007;114:921–6.
47. Feuer WJ, Budenz DL, Anderson DR, *et al*. Topographic differences in the age-related changes in the retinal nerve fiber layer of normal eyes measured by Stratus optical coherence tomography. *J Glaucoma* 2011;20:133–8.
48. Knight OJ, Girkin CA, Budenz DL, *et al*. Effect of race, age, and axial length on optic nerve head parameters and retinal nerve fiber layer thickness measured by Cirrus HD-OCT. *Arch Ophthalmol* 2012;130:312–18.
49. Ooto S, Hangai M, Tomidokoro A, *et al*. Effects of age, sex, and axial length on the three-dimensional profile of normal macular layer structures. *Invest Ophthalmol Vis Sci* 2011;52:8769–79.
50. Kang SH, Hong SW, Im SK, *et al*. Effect of myopia on the thickness of the retinal nerve fiber layer measured by Cirrus HD optical coherence tomography. *Invest Ophthalmol Vis Sci* 2010;51:4075–83.
51. Zou H, Zhang X, Xu X, *et al*. Quantitative in vivo retinal thickness measurement in chinese healthy subjects with retinal thickness analyzer. *Invest Ophthalmol Vis Sci* 2006;47:341–7.
52. Chan CM, Yu JH, Chen LJ, *et al*. Posterior pole retinal thickness measurements by the retinal thickness analyzer in healthy Chinese subjects. *Retina* 2006;26:176–81.
53. Hoh ST, Lim MC, Seah SK, *et al*. Peripapillary retinal nerve fiber layer thickness variations with myopia. *Ophthalmology* 2006;113:773–7.
54. Maroco J, Silva D, Rodrigues A, *et al*. Data mining methods in the prediction of Dementia: A real-data comparison of the accuracy, sensitivity and specificity of linear discriminant analysis, logistic regression, neural networks, support vector machines, classification trees and random forests. *BMC Res Notes* 2011;4:299.
55. Douglas PK, Harris S, Yuille A, *et al*. Performance comparison of machine learning algorithms and number of independent components used in fMRI decoding of belief vs disbelief. *NeuroImage* 2011;56:544–53.